4-1-1996

Dynamics and Conformation of Polymer Chains in a Porous Medium

Grace M. Foo
University of Southern Mississippi

R.B. Pandey
University of Southern Mississippi

D. Stauffer
Cologne University

Dynamics and conformation of polymer chains in a porous medium

Grace M. Foo,[1] R. B. Pandey,[1,2,3] and D. Stauffer[4]
[1]*Program in Scientific Computing,* [2]*Department of Physics and Astronomy*
University of Southern Mississippi, Hattiesburg, Mississippi 39406-5046
[3]*Computational Science Program, National University of Singapore, Lower Kent Ridge Road, Singapore 119260*
[4]*Institute for Theoretical Physics, Cologne University, Zulpicher Strasse 77, D-50923 Cologne, Germany*
(Received 26 October 1995)

Conformational and transport properties of polymer chains in a porous medium are studied using computer simulations. Two types of links between the consecutive nodes of the self-avoiding walk (SAW) chains are considered: (i) constant bond and (ii) flexible (fluctuating) bond. In addition to normal diffusive motion for the global transport of chains, we observe unusual nondiffusive transport phenomena such as subdiffusive power-law dependence of the rms displacement ($R_{\rm rms}$) of the chain with time (t), i.e., $R_{\rm rms}=At^k$ with an exponent k less than 1/2 at low porosity. In two dimensions, we find that the power-law exponent k is nonuniversal as it depends on the barrier concentration (p_b) and the chain length (L_c) with the magnitude of $k\simeq 0.0-0.5$. The chains with flexible bonds exhibit better relaxation with the value of k slightly higher than that for the chains with constant bonds at low porosities. The subdiffusion constant A shows a nonuniversal power-law dependence on the chain length, $A\sim L_c^{-\alpha}$, with $\alpha\simeq 0.28-1.85$ for chains with constant bond, and $0.33-1.27$ for chains with flexible bonds. A similar but less pronounced effect of impurity barriers is also observed in three dimensions. The radius of gyration of the chains is affected by the presence of barriers; characteristics of the crossover from a SAW to collapse conformations are reported, along with the anomalous conformation as a function of barrier concentration.

PACS number(s): 36.20.Ey, 47.55.Mh, 83.10.Nn, 02.70.Lq

I. INTRODUCTION

Understanding the conformational properties and dynamics of chain polymers has been a subject of continued interest for the past few decades [1–4]. The conformation of a polymer chain depends on two factors: the basic nature of the free chain [i.e., random walk (Gaussian), self-avoiding walk (SAW), Levy walk, ballistic walk, etc.] and the medium in which the chain is embedded. It is now well known that the conformation of a polymer chain is a SAW in a good solvent, a Gaussian at the θ point, and a collapse configuration in poor solvent, while it is Gaussian even in a good solvent in melt [3]. Most of the studies are focused on evaluating one of these standard conformations and the crossover from one conformation to another. Very little attention is given to anomalous conformations [5] of the chains that may result from various factors such as the nature of the host media, the interactions, and the temperature, etc. We study the effects of the heterogeneity of the medium on the conformation of the chains.

The effect of heterogeneity on the dynamics of chains [3,4] is even more difficult. The power-law dependence of the monomers and the center of mass of the chains on time has been one of the most debated subjects in the area of polymer physics for over a decade [4,6–14]. In particular, the crossover between Rouse (local motion of internal nodes at short time, nonentangled regime) to reptation (the motion of nodes in a highly entangled regime) power-law behavior has been controversial and has generated intense activities. The notion of reptation for the dynamics of chains and its dominant role in the long time regime seems more acceptable now primarily due to the progress in computing with the large-scale simulations [11–14]. In recent years, computer simulations have become one of the most powerful tools in investigating the conformational properties and dynamics of chain polymers [14], which are too complex to handle by analytical theoretical methods [4]. These problems become more complex as we incorporate features such as interactions between the polymers and solvents and the effects of barriers. We restrict ourselves here to the effects of quenched barriers and the excluded volume interactions of the polymer chains. Furthermore, we will use both internal kink-jump and reptation to move the chains. We know [15] that the reptation destroys the correct local dynamics, and therefore the Rouse-like dynamics is not expected. Without the reptation, on the other hand, it will be very difficult to reach the asymptotic regime to address the issues related with the long time behavior with presumably equilibrated chain lengths in steady state.

The transport properties of even the structureless particles, i.e., the interacting lattice gas in the presence of barriers, are very difficult to investigate [16–18]. The motion of noninteracting particles (i.e., single particle) in random media such as a percolating system [19,20] is, however, well understood [21–26]. The asymptotic power-law behavior of the random walk motion of a particle in a percolating medium becomes anomalous [26] at the percolation threshold where the ramification of the host space becomes very high. The everlasting competition between the random walk movement of a particle and the stochastic geometry of the inhomogeneous medium with infinite percolation correlation length [19,20] leads to such unusual transport behavior. It may be argued [5] that the conformation and dynamics of chains in melt should share this feature in certain time regimes.

The relaxation times associated with the conformations of

the chains and their motion and with the host medium may cause more difficulties for chains [27] than that for a diffusing particle. It can be realized by considering the motion of a tagged (tracer) chain in the melt where the remaining chains constitute the host medium. The chains other than the tagged chain constitute the medium. The tracer chain moves and explores its conformation in a limited host space — the cage [3]. On average, the volume of the cage is the size of the typical pore space (the volume of the system minus the volume of the polymer chains) per chain. The relaxation time of the chain to explore all its conformational configurations (τ_{c1}) and to approach its power-law motions (τ_{t1}) depends on the shape and size of the cage, which itself depends on time since all the chains are mobile. Thus, at least for the power-law transport, we have to deal here with two relaxation times: τ_{t1} for the chains and τ_2 for the cage. If $\tau_2 \gg \tau_{t1}$, then one may treat the cage as a quenched medium; a static percolating medium could be such a cage in the extreme limit ($\tau_2 \to \infty$). We present here a computer simulation study of the conformational properties and dynamics of chains in the presence of quenched barriers, i.e., a porous medium.

Several attempts have been made in recent years to understand the conformation and dynamics of polymer chains in quenched random media [28–34]. Using an analytic treatment with the n-replica method, Muthukumar [28] has shown that the chains conform to SAW and random walk (RW) conformations in the weak and intermediate impurity concentration regimes while the radius of gyration depends on the concentration in the high concentration regime. Using an effective field theory, Haronska and Vilgis [33] have argued that, in the presence of strong quenched disorder, the size of the chain is independent of its contour length, and it depends on a measure of disorder. The type of heterogeneous media and smoothing out of heterogeneities in averaging the physical quantities, i.e., radius of gyration, in such analytical methods may not capture the intricate details (i.e., nonlinearity of the heterogeneous media) of all impurity distributions, i.e., a percolating medium as in computer simulations. We study the conformation and dynamics of chain polymers in a quenched random system and observe some unusual power-law dependence of the rms displacement of chains with time and that of the radius of gyration with the mass of the chains.

Using computer simulations, Baumgärtner and Muthukumar [29] have studied the conformational and transport properties of chains in a random system modeled by percolation [19,20]. They do not consider excluded volume interactions in modeling the chains. The important effect of random barriers in their study is the observation of the crossover from a Gaussian to a collapse state of the radius of gyration on increasing the barrier concentration. We will study the conformation and transport properties of SAW chains in a porous medium generated by a random distribution of impenetrable quenched barriers as in percolation. We consider two types of chain models: (1) constant bond and (2) flexible bond (bond fluctuation) between the consecutive nodes [35]. These simulations are carried out in both two and three dimensions. The simulations in three dimensions are useful in understanding the viscoelastic properties of polymer chains in melt and in porous gel. Furthermore, most of the analytical and computer simulation studies have been carried out in three dimensions and therefore it is relatively easier to see how the physical properties of the SAW chains in our model are modified by the quenched impurities. Although the model chains can describe the motion of polymers in dilute gels better than the effective sphere models [36], they may still be far from describing the laboratory polymers, say linear polystyrene in the matrix of cross-linked polymers [37]. Enormous efforts have been recently devoted to studying the transport and conformation of polymers experimentally, and in electrophoretic processes in particular [38]; this is another important area of modeling [39,40], which will not be considered here. Nevertheless, studying the conformation and dynamics of chains in porous media (even without a driving field as in electrophoresis) is very important in understanding such complex systems.

The motivations for our study in two dimensions are the following: it is relatively easier to investigate and check the conformation of the chains on a square lattice despite large fluctuations in lower dimensions. A difficulty on the square lattice may be encountered due to the possibility of some nonergodic conformations for the SAW [14]. However, the probability of such a conformation is too small to affect our results on the power-law dependence of the rms displacement of the chains on time or that of the radius of gyration on the contour length. The nonergodicity due to conformational trapping can be monitored in our simulations. The restrictions in conformational configurations may, nevertheless, be caused by the presence of impurity barriers and other factors such as polymer concentration and temperature, which may lead to nonergodicity. Thus, some degree of "frustration" [41] may not be undesirable in such simulations. Simulations in two dimensions may have some applications in coating flow and paint [42], where conformation and dynamics of the polymer on a surface are important in understanding the stability of paint. To our knowledge, there is no such study on the basic conformational and dynamic properties of chains on a heterogeneous surface that is presented here. In the following section we will introduce the model. The physical quantities are defined in Sec. III. The results for the transport and the conformational properties are presented in Secs. IV and V, respectively, with a summary in Sec. VI.

II. MODEL

A. Lattice initialization

We consider a discrete lattice of size L^d, where d is the dimension [square lattice ($d=2$) and cubic lattice ($d=3$)], and have two ways to initialize it: (a) A fraction p_b of the lattice sites is randomly occupied by quenched barriers with one barrier at a site. A number of chains n_c each of length L_c, of a fixed concentration p_c, are then placed randomly in the pore space. In order to place a chain of length L_c, we select an initial pore site randomly. Then, consecutive nodes are placed at randomly selected nearest neighbor sites with the following constraints: (1) the chains are nonintersecting, similar to a constrained self-avoiding walk; (2) two chains cannot occupy the same lattice site; and (3) a chain cannot cross over the barrier. If the attempt to place the entire chain (i.e., the L_c+1 nodes) fails then choose another empty initial site randomly and repeat the above process. If the concentra-

tion of the barriers is high, then it is difficult to place many chains of large lengths in particular. Therefore, we use a fixed number of attempts (usually large) to place the chains in pores. The maximum number of chains (a jamming coverage [43]) that can be placed into the pores with our fixed number of attempts may be smaller than the preassigned number of chains n_c and in that case the value of n_c is updated to the actual number of chains generated. Thus, we may not have control over the precise concentration of chains in this method. (b) There is a way to get around the difficulty in placing the preassigned number of chains by packing the chains first regularly in the lattice and then placing the barriers. The initial chain configurations will not be random as in the above process (a) and it will take more time to equilibrate such initial configurations. Therefore, instead of placing the chains regularly, we can distribute them randomly in sequence (random sequential initialization). Since the barriers are structureless (lattice points), it is relatively easier to drop them into the lattice after placing the chains in a constrained SAW growth process. Although we can generate some random configurations, we cannot pack a large number of chains again due to the jamming limit in such random sequential chain growth process. However, we believe that this is a reasonable compromise, and in our study here we have used this method of preparing the samples.

B. Hopping algorithm

We use kink-jump and slithering-snake reptation moves for the chain dynamics. As mentioned before, we consider two types of chains: (1) chains with constant bonds (links) and (2) chains with flexible bonds. We randomly select a node at site i from the L_c+1 nodes of a chain. If site i is one end of the chain (head or tail), then we randomly select one of its nearest neighbor (nn) sites j. If site j is empty, then the end i moves to site j and the whole chain follows this end, leaving behind an empty site at the other end — the chain reptation thus describes a collective motion of the chain [3,4]. If site i is one of the internal nodes of the chain, then we choose one of its neighboring sites j from a set of its next nearest neighbor (nnn) sites in order to perform local "kink-jump" motion for the chains with constant bonds. If site j is empty, then the node at site i moves to site j without changing its associated bond lengths. For the chains with the flexible bonds, on the other hand, we select one of the neighboring sites (j) from a set of its nearest and next nearest neighbor sites. If site j is empty and happens to be one of the nnn sites, then the kink-jump motion is attempted as in the constant bond model. However, if the empty site j is one of its nn sites, then we attempt to implement an additional local move by stretching or contracting the bonds associated with the node at site i. A typical kink-jump and bond fluctuation is shown in Fig. 1. Note that the bond fluctuation involves only a small change in the bond length in this model. However, this involves evaluation of elastic energy dE associated with the change in the length:

$$dE = k dr^2, \tag{1}$$

where $dr = |r_i - r_{i-1}| + |r_i - r_{i+1}| - |r_j - r_{i-1}| - |r_j - r_{i+1}|$, r_i is the position of the ith node, and k is an elastic constant. If dE is less than or equal to zero then we perform the move.

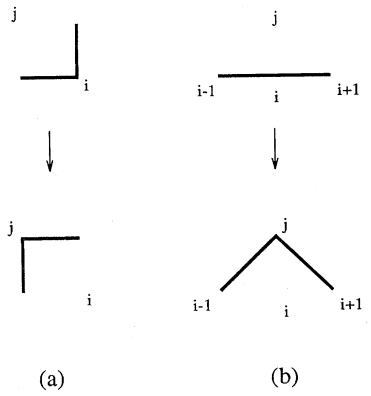

FIG. 1. A kink-jump (a) and a bond fluctuation (b) move.

If dE is greater than zero then we attempt to move with the Boltzmann distribution $e^{-\beta dE}$, $\beta = 1/k_B T$, where k_B is the Boltzmann constant and T is the temperature. Thus we take into account some elastic energy due to stretching of the bonds in local internal motion for the elastic bond model in addition to only its entropic contribution considered in the constant bond model. We would like to point out that our elastic bond fluctuation mechanism is different from the bond fluctuation methods used in the literature [14,35] in which only a constant energy is associated with bond fluctuation of different lengths.

III. PHYSICAL QUANTITIES

We study (a) the transport quantities for the chains [variation of the root mean square (rms) displacements with time] and (b) their conformational property (radius of gyration). At a fixed porosity $p_s = 1 - p_b$, where p_b is the barrier concentration, we keep track of these quantities during the simulation. These quantities are defined in the following:

(a) Displacements of the chains: we evaluate the displacement of each monomer (node) from which we calculate the displacement and rms displacements of the chain and that of its center of mass as a function of time. In order to keep track of limited periodic values of the displacements we store the relevant quantities at equal intervals t_i; thus our total time step $t = t_o \times t_i$, where t_i is the size of the innermost time loop and t_o is the size of outer time loop.

The $x(y)$ component of the displacement $u_{x(y)}$ of a chain in one Monte Carlo time step (MCS) is

$$u_{x(y)} = \sum_{l=1}^{L_c+1} un_{x(y)_l}, \tag{2}$$

where $un_{x(y)_l}$ is the $x(y)$ displacement of each node of the chain in unit time. We also monitor the contribution to displacement due to reptation $(ur_{x(y)})$ and internal kink-jump $(ui_{x(y)})$ separately. The total $x(y)$ displacement of a chain in time t is, therefore,

$$r_{x(y)}(t) = \sum_{k=1}^{t} ur_{x(y)_k}, \tag{3}$$

$$i_{x(y)}(t)=\sum_{k=1}^{t} ui_{x(y)_k}. \tag{4}$$

We define the mean square displacement per chain at time t as

$$\langle r^2_{x(y)}(t)\rangle=\frac{1}{n_c}\sum_{k=1}^{n_c} r^2_{x(y)}, \tag{5}$$

$$\langle i^2_{x(y)}(t)\rangle=\frac{1}{n_c}\sum_{k=1}^{n_c} i^2_{x(y)}, \tag{6}$$

due to reptation and kink-jump motion, respectively. In what follows, we use r and i to describe the contribution due to reptation and internal (kink-jump) motion unless otherwise specified. Thus, the root mean square displacements per chain due to reptation and kink-jump motion in time t are

$$r_{\rm rms}(t)=\sqrt{\langle r^2_x(t)\rangle+\langle r^2_y(t)\rangle}, \tag{7}$$

$$i_{\rm rms}(t)=\sqrt{\langle i^2_x(t)\rangle+\langle i^2_y(t)\rangle}. \tag{8}$$

(b) Radius of gyration: We evaluate the radius of gyration (R_g) of each chain defined by

$$R_g=\frac{1}{N_s n_c(L_c+1)}\sum_{j=1}^{n_c}\sum_{i=1}^{L_c+1}\sqrt{\langle[r_i(j)-r_{cm}(j)]^2\rangle}, \tag{9}$$

$$r_{cm}=\frac{1}{L_c+1}\sum_{i=1}^{L_c+1} r_i, \tag{10}$$

where N_s is the number of independent samples, n_c is the number of chains in each sample, and $r_i(j)$ is the position of

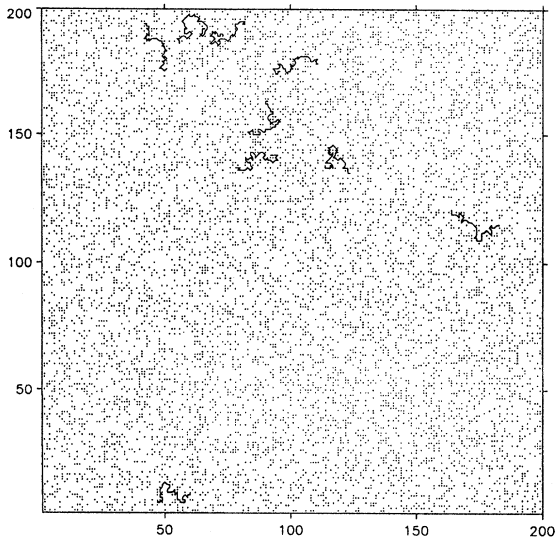

FIG. 2. Snapshot of 200×200 lattice with chains of length 40 and concentration 0.01, and barrier concentration 0.2. Chains are connected sites, barriers are shown by dots, while pores are open.

ith node of the jth chain; $\langle\rangle$ shows the ensemble averaging over configurational states (i.e., over MCS time). This quantity is averaged over the number of chains and samples to obtain a reliable estimate.

The parameters in this study are the concentration of barriers (p_b) (or porosity $p_s=1-p_b$) and chain length (L_c) for chains with constant and fluctuating bonds. For a fixed set of these parameters, we have performed a number of independent simulations to obtain a reliable estimate of the physical quantities. Because of the complexities of the problem, ef-

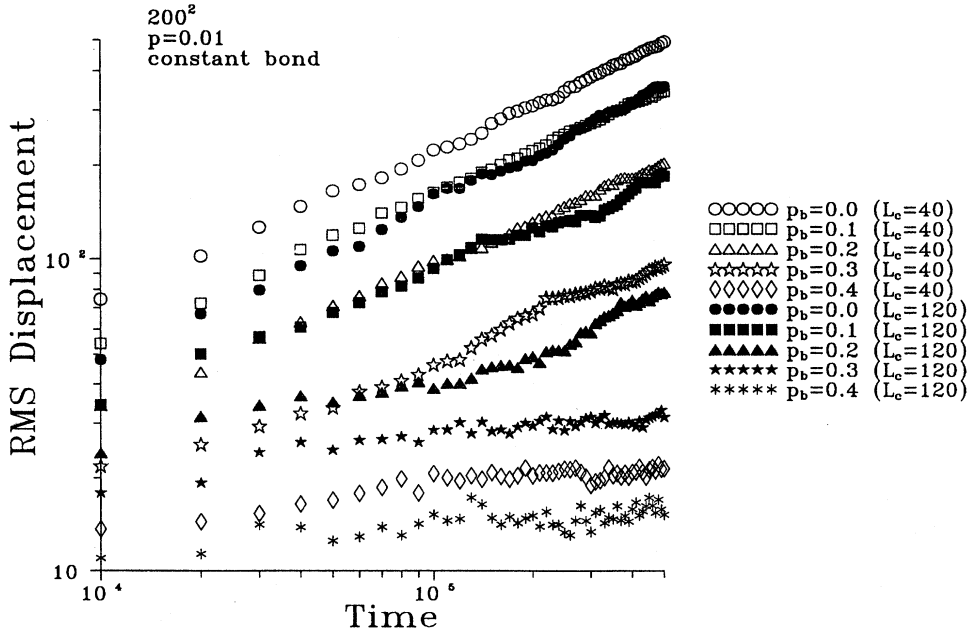

FIG. 3. Log-log plot of rms displacement (end nodes) versus time of constant bond chains, for chain lengths $L_c=40$ and 120 and barrier concentrations $p_b=0.0-0.4$. The lattice size was 200×200 with 30 independent samples.

TABLE I. Exponent k for chains in $2d$ with constant bonds, errors on order of $\simeq 0.03$.

Chain length	p_b 0.0	0.1	0.2	0.3	0.4
20.0	0.51	0.49	0.49	0.50	0.31
40.0	0.51	0.47	0.46	0.45	
80.0	0.49	0.48	0.50	0.15	
120.0	0.54	0.41	0.41		
160.0	0.49	0.47	0.34		

forts have been made to obtain as many independent samples as permitted by the available resources. These simulations are CPU intensive (about 6000 CPU hours on CRAY YMP, CRAY T3D, SUN, IBM workstations and Pentiums). In many instances, we have substantial fluctuations in the data where it is very hard to provide a definite prediction while there are cases where there will be clear evidence for a certain dependence of these quantities on the independent variables. In the following we present results on these quantities.

IV. TRANSPORT QUANTITIES

The variations of the rms displacements of each chain with time are studied as a function of barrier concentration for both chain types with constant and fluctuating bonds. We use both kink-jump and "slithering-snake" (reptation) motions to study the transport of the chains. In principle, there may be a variety of kink-jump and crankshaft movements involving various numbers of bonds with different modes. We have, however, considered only the lowest order of kink-jump movement involving two consecutive bonds. Such local dynamics is important in relaxing the chain conformations. The reptation moves, on the other hand, dominate the global transport of a chain involving its cooperative motion. Therefore, the nature of the variation of the rms displacement of chains with time should be determined by analyzing the displacement of chains due to reptation alone. The displacement due to internal kink-jump motion, in combination with the reptation, may sometime lead to spurious power-law dependence, particularly in a porous medium for some bond-fluctuating chains, as we will see below. We will, therefore, restrict ourselves to the reptation component of the rms displacement of the chains to study the effects of quenched disorder on its power-law dependence on time.

A. Two dimensions

We have used lattices of size 200×200 for our simulations with chain lengths in the range $L_c=40-160$. The barrier concentration is varied with $p_b=0.0-0.4$, so the porosity, the fraction of open sites that form the pores, $p_s=1-p_b$, ranges from 1.0 to 0.6. Note that the percolation threshold for site percolation in two dimensions is about 0.593 [19]. For a fixed value of porosity and chain length, we have used 30 independent runs to obtain the average physical quantities. A snapshot of a sample configuration after 500 000 steps is shown in Fig. 2.

1. Constant bond

Figure 3 shows the rms displacement versus time plots for various values of the barrier concentrations and for the chain lengths 40 and 120 with constant bond. Obviously, these data are fluctuating, and at higher values of p_b ($p_b\geq0.4$) it is rather difficult to see if the chains have global transport.

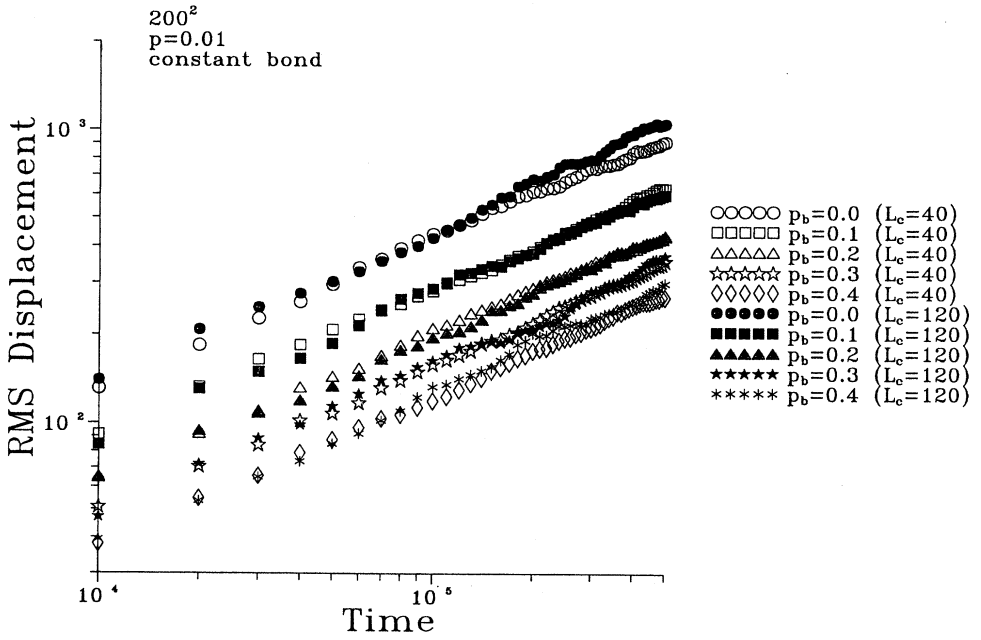

FIG. 4. Log-log plot of rms displacement (internal nodes) versus time of constant bond chains, for chain lengths $L_c=40$ and 120 and barrier concentrations $p_b=0.0-0.4$. Same statistics as in Fig. 3.

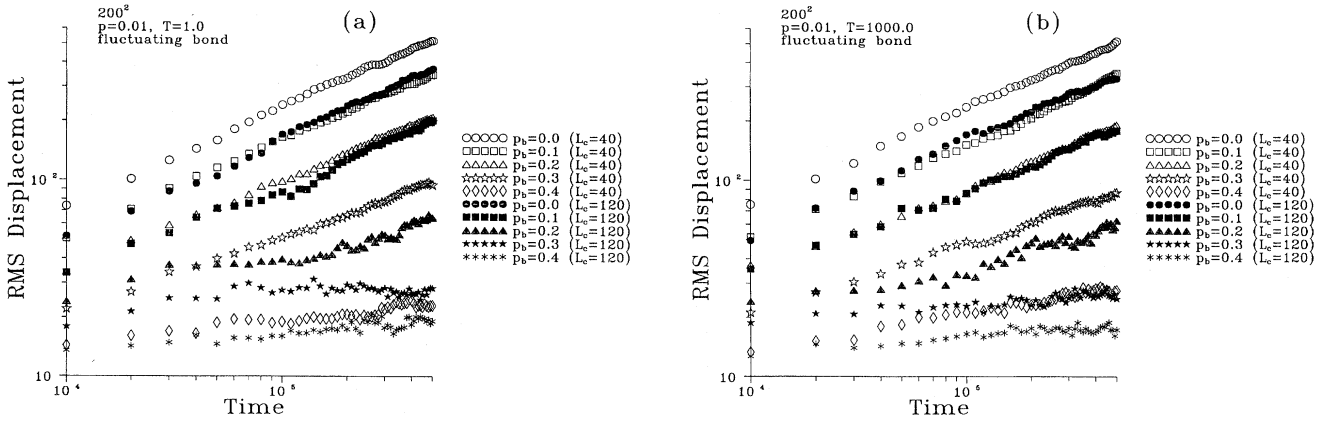

FIG. 5. Log-log plot of rms displacement (end nodes) vs time of fluctuating bond chains at (a) $T=1.0$ (b) $T=1000.0$, for chain lengths $L_c=40$ and 120 and barrier concentrations $p_b=0.0-0.4$. The lattice size was 200×200 with 30 independent samples.

However, it is clear that the nature of the temporal variation of the rms displacement of the chains seems to depend strongly on the concentration of the barriers. Let us assume a power-law dependence for the rms displacement of the chain with time,

$$R_{\rm rms}=At^k, \tag{11}$$

where A is a constant and k is the power-law exponent. Table I shows a complete set of our estimate of k for various values of p_b and L_c. We see that for the chain length $L_c=20, k\simeq 1/2$ at $p_b=0.0-0.3$, $k\simeq0.31$ at $p_b=0.4$, while for $L_c=80$, the estimate of k drops down to 0.15 even at $p_b=0.3$ and becomes vanishingly small for $p_b\geqslant0.4$. We note that the data for the longer chains are more fluctuating than that for the shorter chains for the same number of independent samples. This is not unreasonable, since the conformational relaxation of the larger chains is more severely hindered by the barriers at the pore boundaries than that for the shorter chains, which are relatively less spread. Despite the fluctuations, we observe that the exponent k depends on the barrier concentration p_b and perhaps on the chain length L_c, especially at higher barrier concentrations $p_b\geqslant0.2$ (see Table I).

We would like to point out that the random walk of a particle in a quenched random system becomes anomalous at the percolation threshold [19,20]; the everlasting competition between the random walk and stochastic geometry of the percolating network at the percolation threshold leads to such subdiffusive power-law behavior [21–26]. The stochastic motion of a SAW chain in a stochastic geometry [44] is more complex due to interplay between the conformational stochastic relaxations and the competition between the chain transport and the stochastic geometry. Although our data appear somewhat fluctuating, the trend is clear within the framework of the above arguments. At barrier concentrations $p_b\geqslant0.2$, the power-law exponent k is nonuniversal in a sense that it depends on both p_b and L_c. Thus, we tend to believe that the motion of the chains is not only subdiffusive, but is quite different from that of Rouse-like motion and reptation [4] in a quenched porous medium.

One would like to see the temporal variation of the rms displacement due to lateral movement (hopping) of the inter-

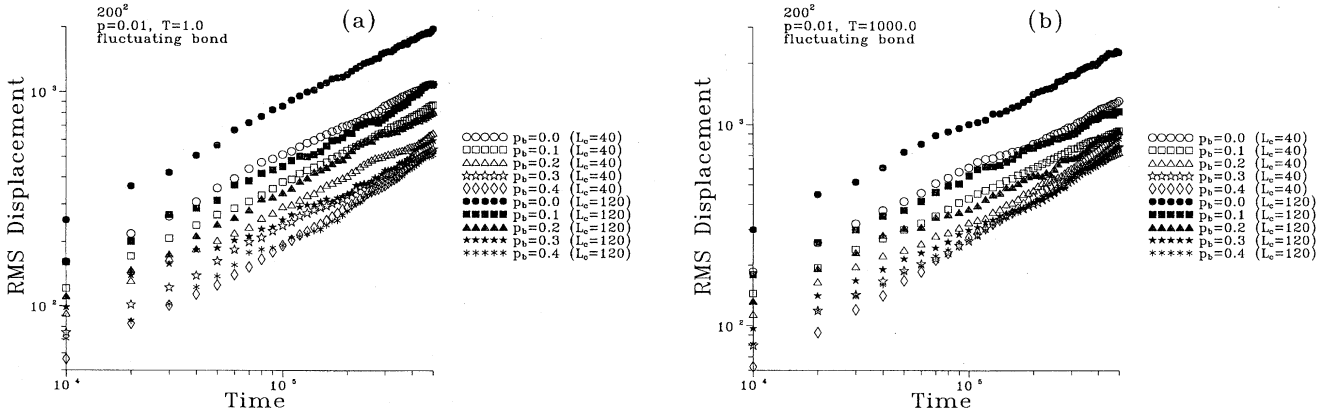

FIG. 6. Log-log plot of rms displacement (internal nodes) vs time of fluctuating bond chains at (a) $T=1.0$ and (b) $T=1000.0$, for chain lengths $L_c=40$ and 120 and barrier concentrations $p_b=0.0-0.4$. Same statistics as in Fig. 5.

TABLE II. Exponent k for chains in $2d$ with fluctuating bonds, $T=1.0$, errors on order of $\simeq 0.03$.

Chain length	p_b 0.0	0.1	0.2	0.3	0.4
20.0	0.52	0.49	0.49	0.45	0.32
40.0	0.49	0.48	0.47	0.41	0.13
80.0	0.54	0.52	0.41	0.33	
120.0	0.52	0.52	0.30		
160.0	0.45	0.45			

nal nodes in the kink-jump motion. Figure 4 shows such a plot for two chain lengths ($L_c=40$ and 120) at various barrier concentrations. One would immediately note that these data are less fluctuating than the corresponding data for the collective transport due to reptation. The kink-jump motion involves many more nodes (L_c-1) than the two nodes at the chain ends in reptation. The stochastic internal movements ("flipping") of these nodes are independent of each other. Therefore, the statistics is improved. The slopes of the rms displacement with time on the log-log scale (Fig. 4) is about 1/2. Thus, the stochastic internal flipping is diffusive.

2. *Fluctuating bonds*

We consider a bond fluctuation in which the bond length between the consecutive nodes may fluctuate by a small amount (between 1 and $\sqrt{2}$) as the node moves [see Fig. 1(b)]. The bond fluctuation involves elastic energy and the moves are accepted by sampling the change in elastic energy by a Boltzmann distribution at a fixed temperature T in units of Boltzmann constant (see Sec. II B). Figures 5 and 6 show the variation of the rms displacement of the chains due to reptation and kink-jump movements, respectively, at temperatures $T=1$ and 1000. We try to analyze the power-law behavior using Eq. (11). The estimate of the power-law exponent k for the rms displacement due to reptation is presented in Tables II and III, as a function of the chain length and the barrier concentration. The reptation motion of the polymer chains shows subdiffusive behavior at higher concentration of barriers as in the case of chains with the constant bond discussed above. The characteristic barrier concentrations at or above which such a subdiffusive power-law behavior occurs seem to depend on the chain length — the higher the chain length, the lower the characteristic barrier concentration (see Tables II and III). The rms displacement due to kink-jump motion, on the other hand, shows a diffusive behavior at low barrier concentrations, and a faster superdiffusive ($k>0.5$) and driftlike ($k=1$) motion at high barrier concentrations ($p_b=0.6$) (see Fig. 6). However, we seem to understand this superdiffusive behavior of the chains (see below). We know that the chains have relatively more freedom to relax with the bond fluctuations than with the constant bonds. Therefore, the probability of the entropic trapping is smaller with our bond fluctuating model. Note that there is no significant difference due to temperature in the variation of the rms displacement of chains with time (see Figs. 5 and 6). This is due to the fact that the temperature affects only the bond stretching as the internal node attempts to move to its neighboring site — such moves seem to be very limited in comparison to all other moves without stretching due to limited use of the temperature dependent Boltzmann factor.

TABLE III. Exponent k for chains in $2d$ with fluctuating bonds, $T=1000.0$, errors on order of $\simeq 0.03$.

Chain length	p_b 0.0	0.1	0.2	0.3	0.4
20.0	0.46	0.47	0.48	0.41	0.25
40.0	0.47	0.52	0.48	0.38	0.18
80.0	0.51	0.49	0.48	0.29	
120.0	0.45	0.46	0.33		
160.0	0.43	0.41	0.18		

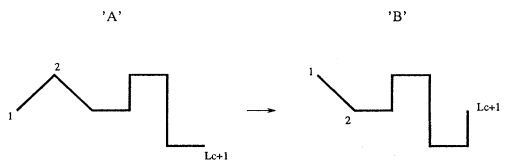

FIG. 7. Reptation and interior motion of fluctuating bond chains.

The driftlike motion of the chains due to kink-jump movements in the restricted pore space can be understood with the following arguments. The chains are executing their stochastic motion with each node selected randomly. Even though the internal nodes are selected more often than the ends (head or tail), there is a finite probability that the mixing of reptation with the kink-jump may eliminate some of the kink-jump configurations. For example, suppose an internal node (say the second node) of a chain has completed a kink-jump motion with bond fluctuation (a configuration A) then followed by a reptation move of the (L_c+1)th node (a configuration B) (see Fig. 7). Since the whole chain follows the (L_c+1)th node, the kink-jump configuration A associated with the second node will be eliminated. The second node may, therefore, be unable to kink-jump back to its original position in configuration A had it attempted to move. Thus, the elimination of the kink-jump conformations such as this, and the high probability of kink-jumps, accelerate the chains. In this process, the chains have moved much larger distance than the pore size as if the chains move around in a "circle" again and again for a long time. This may lead to superdiffusive behavior at high barrier concentrations (i.e., $p_b=0.6$) where the pores are relatively small. Such spurious power-law dependence may also appear in a homogeneous lattice, if the chains are allowed to move around distances

TABLE IV. Average exponent k ($L_c=100$ and 120) for chains in $2d$.

Barrier concentration	Constant bonds	Fluctuating bonds $T=1000.0$
0.0	0.51	0.46
0.1	0.44	0.47
0.2	0.42	0.39

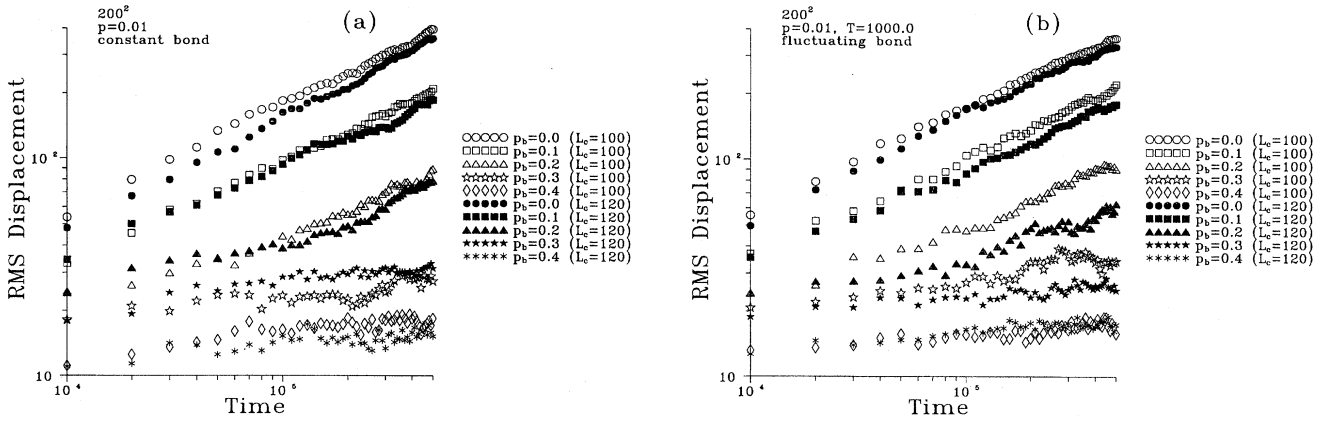

FIG. 8. Log-log plot of rms displacement (end nodes) vs time of (a) constant bond chains and (b) fluctuating bond chains at $T=1000.0$, for chain lengths $L_c=100$ and 120 and barrier concentrations $p_b=0.0-0.4$. The lattice size was 200×200 with 30 independent samples.

much larger than the size of the lattice.

From the above figures (3 and 5 in particular), it is hard to avoid considering ways to reduce fluctuations in the data. To that end, we attempt to improve the statistics by combining the data already obtained for the displacements of two different chain lengths, say L_{c_1} and L_{c_2}. Although this is not an ideal approach, it is worth considering. For a fixed difference in chain length $\Delta L_c=L_{c_1}-L_{c_2}$, the fractional difference in the length $2\Delta L_c/(L_{c_1}+L_{c_2})$ is smaller for the larger chains. Therefore, we consider combining the data for our large chain lengths, $L_{c_1}=100$ and $L_{c_2}=120$. The variation of the rms displacement with time of the combined data, due to reptation motion alone, is shown in Fig. 8(a) for the constant bonds and Fig. 8(b) for the fluctuating bonds. Note that the data for the two chain lengths are quite similar. The least square fits of these data, however, provide a better estimate for the power-law exponent k defined in Eq. (11). The estimate of k at various barrier concentration for the average of both chain lengths is presented in Table IV. We see that k varies with the concentration, about 0.5 at $p_b=0.0$ to 0.39 at $p_b=0.2$ for chains with fluctuating bonds, and to 0.42 at $p_b=0.2$ for chains with constant bonds. This confirms our previous assertion that the rms displacements of chains are subdiffusive in the presence of quenched barriers and that the value of the subdiffusive power-law exponent depends on the barrier concentration. In order to illustrate the dependence of the power-law behavior on chain length and the barrier concentration, we present the variation of the rms displacement with time in Fig. 9 for various chain lengths at $p_b=0.1$ and 0.3. From visual inspection, it is evident that the power-law behavior becomes subdiffusive, at much lower k, for the motion of relatively larger chains at $p_b=0.3$, i.e., $L_c=80$, 120, and 160.

For nondiffusive power-law behavior (i.e., where $k\neq0.5$), we may call the prefactor A [in Eq. (11)] a subdiffusion constant rather than a diffusion constant (D) which is traditionally defined [7] as $D=R_{\rm rms}^2/t$, apart from a numerical factor of order unity. We estimate the value of the prefactor A of the nondiffusive power-law behavior of the chains in our model. The variation of A with the chain length is shown in Fig. 10 for various barrier concentrations. In analogy with the reptation behavior [7], we attempt to ana-

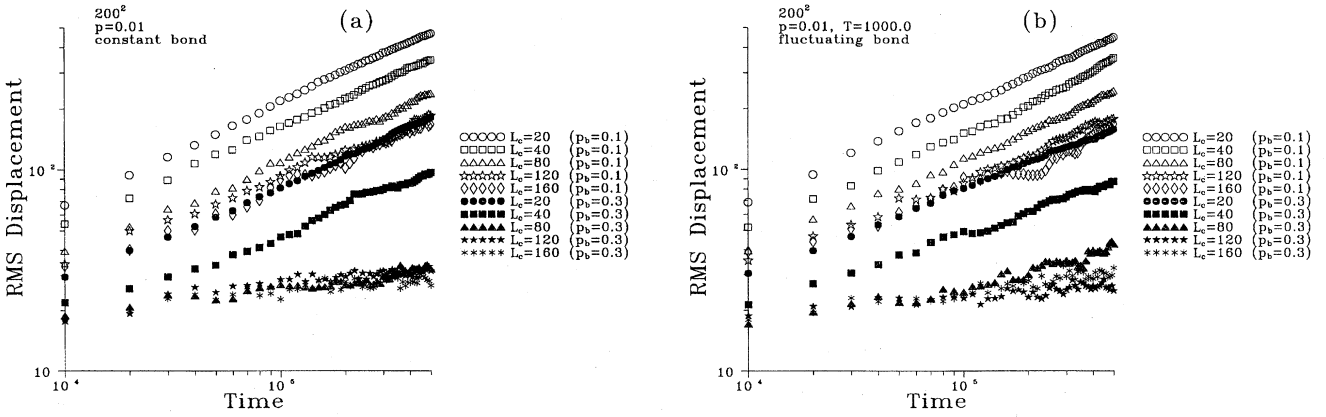

FIG. 9. Log-log plot of rms displacement (end nodes) vs time of (a) constant bond chains and (b) fluctuating bond chains at $T=1000.0$, for chain lengths $L_c=20-160$ and barrier concentrations $p_b=0.1$ and 0.3. Same statistics as in Fig. 8.

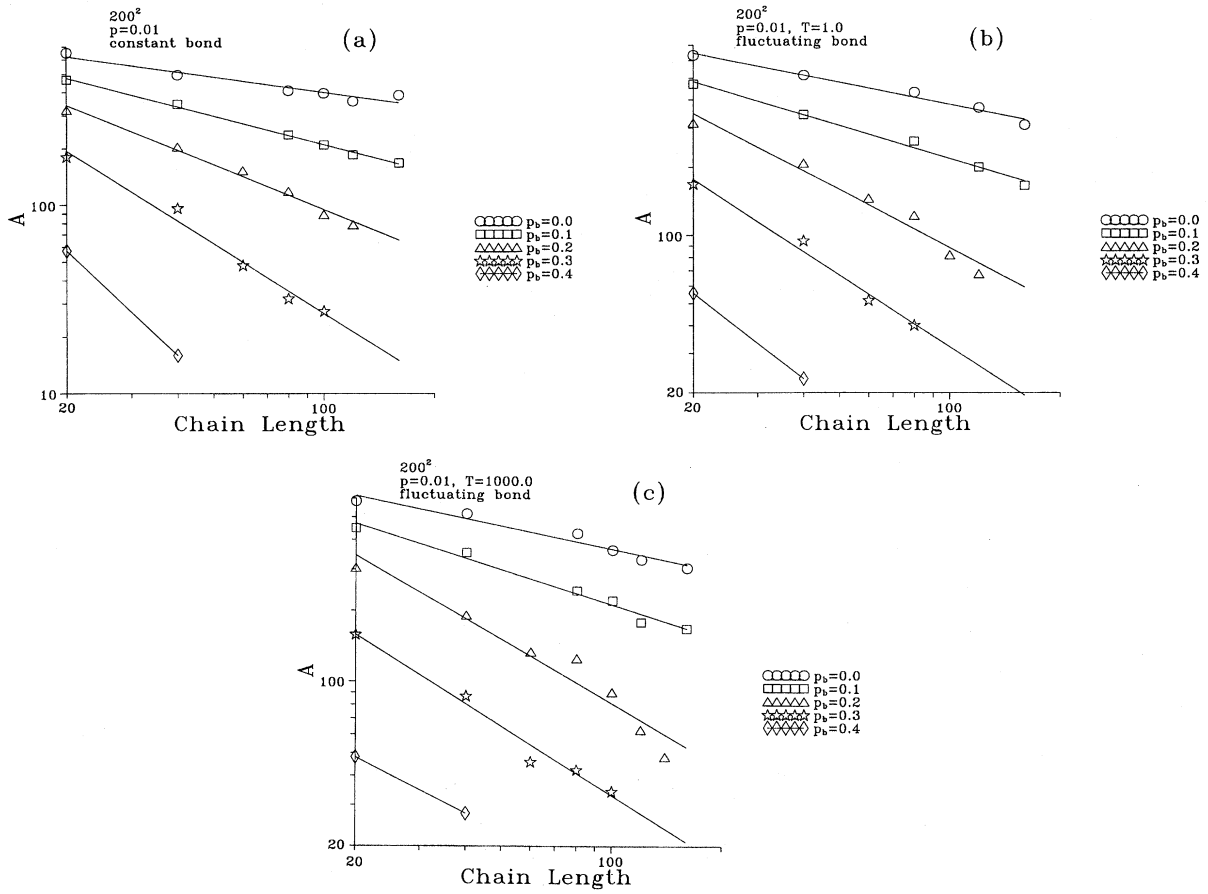

FIG. 10. Prefactor A vs chain length of (a) constant bond chains, and fluctuating bond chains at (b) $T=1.0$ and (c) $T=1000.0$, and barrier concentrations $p_b=0.0-0.4$. Same statistics as in Fig. 9.

lyze a power-law behavior, $A\sim L_c^{-\alpha}$. The estimates of the exponent α are presented in Table V. We observe a strong dependence of this exponent on the barrier concentration. Furthermore, these data indicate that the subdiffusion constant A may depend on the nature of the bond. For example, for chains with constant bonds, $\alpha=0.28-1.85$, while for chains with fluctuating bonds at $T=1.0$, $\alpha=0.33-1.27$, the barrier concentration $p_b=0.0-0.4$. Thus, we find that the subdiffusion constant shows a power-law dependence on the chain length; the power-law exponent depends on the barrier concentration and the type of chain. The nonuniversal nature of the exponent α may be further evidence that the motion of the chains in a quenched porous medium considered here is quite different from the standard Rouse, reptation, or diffusionlike behavior.

B. Three dimensions

In three dimensions, the chains are not as restricted as in two dimensions. The chains have access to more neighboring

TABLE V. Exponent α for chains in $2d$ and $3d$.

Barrier concentration	Constant bonds	Fluctuating bonds		Constant bonds	Fluctuating bonds
		$T=1.0$	$T=1000.0$		$T=1000.0$
	($2d$)	($2d$)	($2d$)	($3d$)	($3d$)
0.0	0.28	0.33	0.32	0.37	0.43
0.1	0.51	0.49	0.49	0.47	0.49
0.2	0.79	0.85	0.90	0.57	0.53
0.3	1.23	1.06	0.97	0.70	0.63
0.4	1.85	1.27	0.80	0.90	0.86
0.5				1.07	1.05

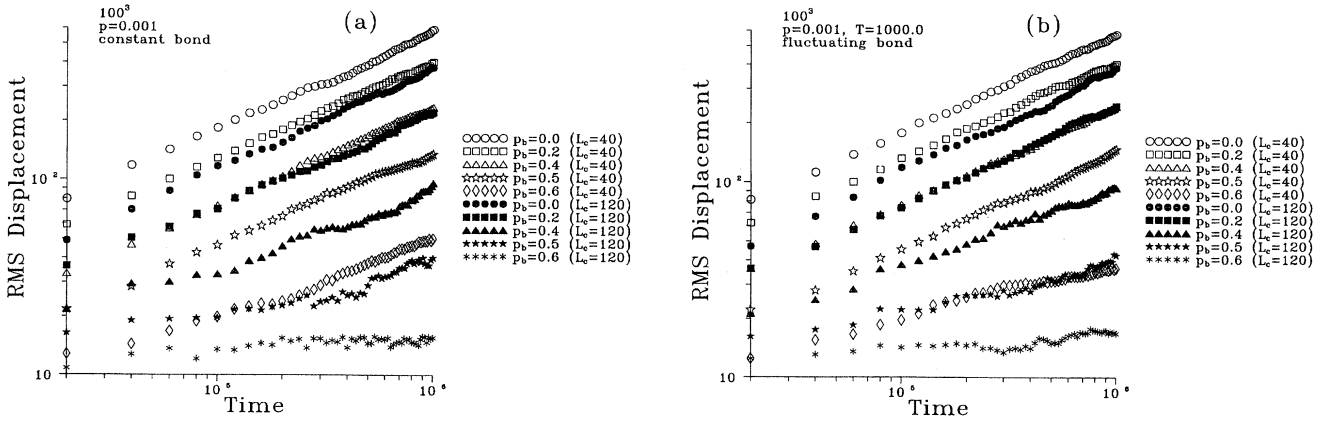

FIG. 11. Log-log plot of rms displacement (end nodes) vs time of (a) constant bond chains, and (b) fluctuating bond chains at $T=1000.0$, for chain lengths $L_c=40$ and 120 and barrier concentrations $p_b=0.0-0.6$. The lattice size was $100\times100\times100$ with 10 independent samples.

sites with coordination number six for both local hopping (kink-jump) and cooperative global (reptation) motion. Therefore, the chains would relax and move comparatively more easily in three dimensions than in two dimensions at the corresponding barrier concentrations and chain lengths. Consequently, one would expect comparatively fewer fluctuations in the data here. The simulations were performed on lattices of typical size $100\times100\times100$, with chain lengths in the range $L_c=40-160$. For each parameter set, about 10 independent runs were used to obtain average physical quantities.

The variation of the rms displacements with time of the constant and fluctuating bond chains are shown in Fig. 11 for various barrier concentrations and chain lengths. The volume fraction of the pores, i.e., the porosity, $p_s=1-p_b$. Therefore, the barrier concentration p_b should be sufficiently high to generate pores with a wide distribution of narrow channels since the percolation threshold is about 0.312 for site percolation [19]. We have considered $p_b=0.0-0.6$ (i.e., $p_s=1.0-0.4$) in this study. We observe that at the low barrier concentrations ($p_b=0.0$ and 0.2), the rms displacements exhibit a diffusive behavior (with slope 1/2). This implies that the barriers impose no restrictions whatsoever as far as the asymptotic behavior of the rms displacements is concerned. However, on increasing the barrier concentrations to $p_b=0.4$ we begin to see the onset of crucial effects on the global motion. Our estimates for the exponent k are shown in Tables VI and VII for constant and fluctuating bond chains, respectively.

We observe a crossover in the power-law behavior at a characteristic time t_c, from a subdiffusive power-law behavior in the short time regime to a diffusive power-law behavior in the long asymptotic time regime. The characteristic time t_c seems to depend on both the chain length as well as on the barrier concentration. Note that t_c increases on increasing the chain length and/or increasing the barrier concentration. This is plausible, as the longer chains hit the barriers at the pore boundaries in a relatively short time in comparison to shorter chains in the same pore. Similarly, increasing the concentration of the barriers reduces the pore size, and therefore, the chains begin to encounter the barriers at the pore boundaries in a relatively shorter time. The competition between the stochastic global hopping of the chains and the barriers leads to an asymptotic subdiffusive power-law behavior ($t_c\to\infty$). This power-law exponent (k) is nonuniversal as it depends on the chain length as well as the barrier concentration. We believe that this is due to a delicate balance between the stochastic conformations of the chains and the interplay between the competing effects of the barriers and the chains motion. Isolating the effects of chain length and barriers and quantifying their predictions will require orders of magnitude more computing resources, and may be carried out when such resources become available in the future.

The effect of the barriers on the rms displacement of the internal nodes due to kink-jump movement is relatively small (see Fig. 12). The rms displacement shows nearly a diffusive motion. The chains with different lengths seem to move together in the presence of barriers. Although the pore boundaries enforce the transverse hopping of the chains, the rms displacement, nevertheless, remains diffusive.

TABLE VI. Exponent k for chains in $3d$ with constant bonds, errors on order of $\simeq0.03$.

Chain length	p_b 0.0	0.1	0.2	0.3	0.4	0.5	0.6
40.0	0.50	0.47	0.49	0.48	0.50	0.44	0.44
80.0	0.45	0.49	0.48	0.52	0.53	0.41	0.14
120.0	0.52	0.46	0.49	0.49	0.41	0.33	
160.0	0.53	0.44	0.53	0.45	0.40	0.15	

TABLE VII. Exponent k for chains in $3d$ with fluctuating bonds, $T=1000.0$, errors on order of $\simeq 0.03$.

Chain length	p_b 0.0	0.1	0.2	0.3	0.4	0.5	0.6
40.0	0.51	0.50	0.49	0.50	0.50	0.49	0.21
80.0	0.49	0.47	0.50	0.53	0.45	0.45	
120.0	0.53	0.50	0.52	0.46	0.39	0.29	
160.0	0.48	0.49	0.53	0.52	0.42	0.17	

To recapitulate the dependence of the power law on chain length and barrier concentration, we present a rms displacement versus time plot in Fig. 13 for various chain lengths $L_c=40-160$ at $p_b=0.2$ and 0.5. Visually, this shows a clear crossover to a subdiffusive behavior at higher p_b.

Note that our data appear more fluctuating than that of Muthukumar and Baumgärtner [32]. There are a few differences worth noting: (1) Their simulations are based on the barrier concentration of ~ 0.4, where the pore concentration ~ 0.6 is much above the percolation threshold (0.312) in three dimensions. The porous media may not be as ramified at such a high pore concentration. (2) Even though they consider SAW chains ($h/l=0.9$), cutting the corners of the random geometry formed by the barriers in their off-lattice simulations may smooth out some of the strong nonlinear effects of the media. (3) The restriction on the degree of freedom on chains may be different from ours.

Finally, the variation of the prefactor A [Eq. (11)] with the chain length is presented in Fig. 14 for various barrier concentrations. We see that there is a power-law dependence, $A\simeq L_c^{-\alpha}$, with a power-law exponent α. The estimates of the exponent α are presented in Table V. As in two dimensions, the power-law exponent α depends strongly on the barrier concentration. The bond fluctuation does not affect the exponent as much as in two dimensions. The exponent α increases from about 0.4 to 1.0 on increasing the barrier concentration p_b from 0.0 to 0.5. Thus, contrary to a specific power-law dependence of the diffusion constant (D), $D\simeq L_c^{-2}$, in previous studies [6,7], we find that our prefactor decays with chain length with a nonuniversal exponent α.

V. CONFORMATIONAL PROPERTIES

Now we would like to look at the conformational properties of the chains in the quenched random medium. As the chains execute their stochastic motion, they explore their conformational states. At a fixed barrier concentration, we monitor the size of the chains to see if the chains have reached their equilibrium value. In the quenched system like this, the number of conformational states will be limited due to the presence of barriers. Additionally, there is a small probability of configurational interlocking in two dimensions [14]. Some degree of frustration [27] in conformational phase space cannot be ruled out. Thus, our equilibrium state here means an approach to a nearly constant value of the size of the chains.

We study the radius of gyration (R_g) [Eq. (9)] of each chain in both two and three dimensions at various barrier concentrations for various chain lengths. In order to gain an idea about the fluctuations, a typical variation of the radius of gyration with time is shown in Fig. 15. We see that the system has reached equilibrium (i.e., stable mean size) in a rather short time except the long chains ($L_c=160$). For the ensemble averaging, we use data for R_g in the long time regime in which the system has reached its equilibrium.

In homogeneous systems and in polymer melt, the radius of gyration shows a well defined power-law dependence on the number of nodes, i.e., mass $N=L_c+1$:

$$R_g\sim N^{\gamma}. \tag{12}$$

The exponent $\gamma=3/4$ in two dimensions and 0.59 in three

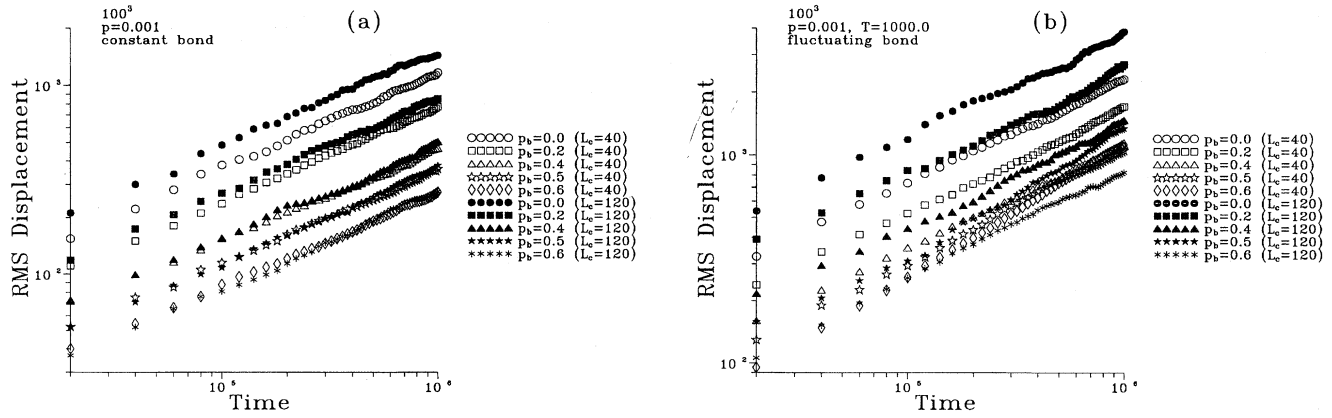

FIG. 12. Log-log plot of rms displacement (internal nodes) vs time of (a) constant bond chains and (b) fluctuating bond chains at $T=1000.0$, for chain lengths $L_c=40$ and 120 and barrier concentrations $p_b=0.0-0.6$. Same statistics as in Fig. 11.

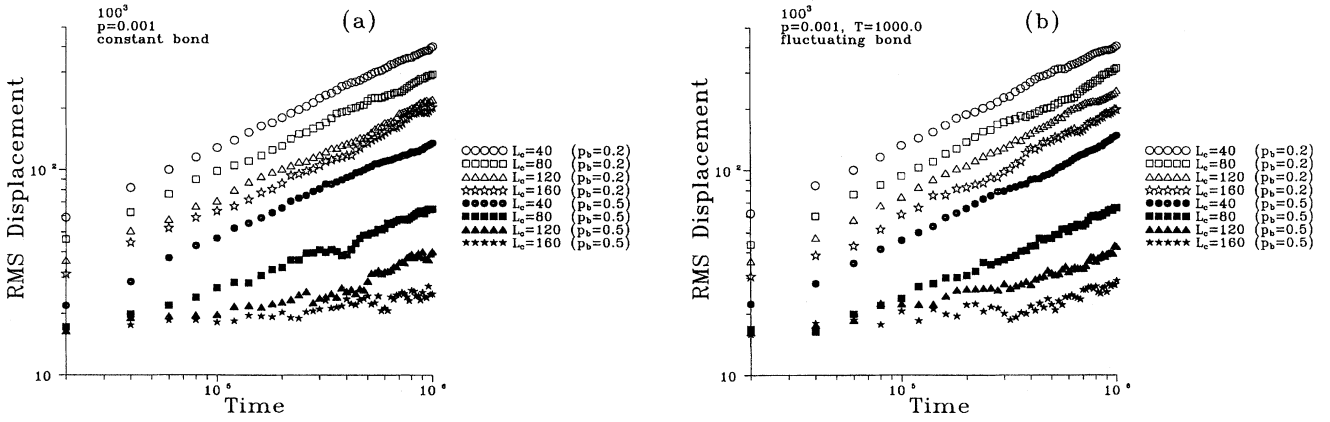

FIG. 13. Log-log plot of rms displacement (end nodes) vs time of (a) constant bond chains and (b) fluctuating bond chains at $T=1000.0$, for chain lengths $L_c=40-160$ and barrier concentrations $p_b=0.2$ and 0.5. The lattice size was $100\times100\times100$ with 10 independent samples.

dimensions for the SAW [3]. We would like to point out that the exponent may depend on the type of matrix [38] in which the chains are embedded (i.e., the concentration of barriers here).

Figure 16 shows the variation of the radius of gyration with the number of links in two dimensions. For the chains with constant bonds, we find that $\gamma\simeq0.68\pm0.03$ for $p_b=0.0-0.3$ and $\gamma\simeq0.59\pm0.01$ at $p_b=0.4$. We see that at the higher barrier concentration ($p_b=0.4$), the size of the chains is relatively smaller than that at the lower barrier concentrations. This trend of reduction in the magnitude of γ on increasing p_b seems to suggest that the chains may collapse to the pore size at high barrier concentration (i.e., low porosity). The corresponding plot for chains with fluctuating bonds is presented in Fig. 17. At $T=1.0$, the exponent $\gamma\simeq0.72\pm0.01$ for $p_b=0.0-0.1$, and $\gamma\simeq0.66\pm0.02$ for $p_b=0.2-0.4$. For the fluctuating bonds at $T=1000.0$, we find that $\gamma\simeq0.71\pm0.03$ for $p_b=0.0-0.3$ and $\gamma\simeq0.62\pm0.02$ at $p_b=0.4$. The data are more fluctuating at the higher barrier concentrations ($p_b\geq0.2$). With the fluctating bond, we note that the effect of p_b on the power-law dependence is less clear at higher p_b ($0.2-0.4$) due to large fluctuations in the data points. At high temperature where the bond fluctuation is more dominant, the data show even more fluctuations.

The variation of the radius of gyration (R_g) with the chain length in three dimensions is shown in Fig. 18. At lower barrier concentrations ($p_b=0.0-0.2$), the exponent $\gamma\simeq0.60$ for both the constant and fluctuating bond chains, with the constant bond chains showing more fluctuation. At higher barrier concentrations ($p_b\geq0.3$), the longer length chains ($L_c\geq120$) are more strongly affected by the presence of the barriers. The decay in the magnitude of the radius of gyration for chains with $L_c\geq120$ suggests that the chains are collapsing and perhaps conforming to the size of the pores, which depends on the barrier concentration. Even though one may have a pore that extends from one end of the sample to another at the barrier concentration, the probability of chains' encounter with the barriers at the pore boundaries is relatively high. Some chains may even be in an isolated pore. In

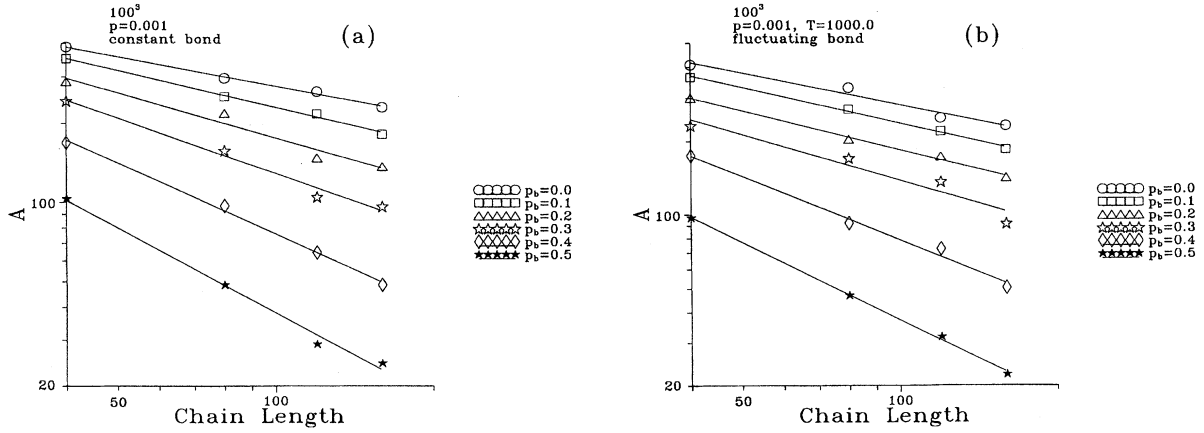

FIG. 14. Prefactor A vs chain length of (a) constant bond chains and (b) fluctuating bond chains at $T=1000.0$ and barrier concentrations $p_b=0.0-0.5$. Same statistics as in Fig. 13.

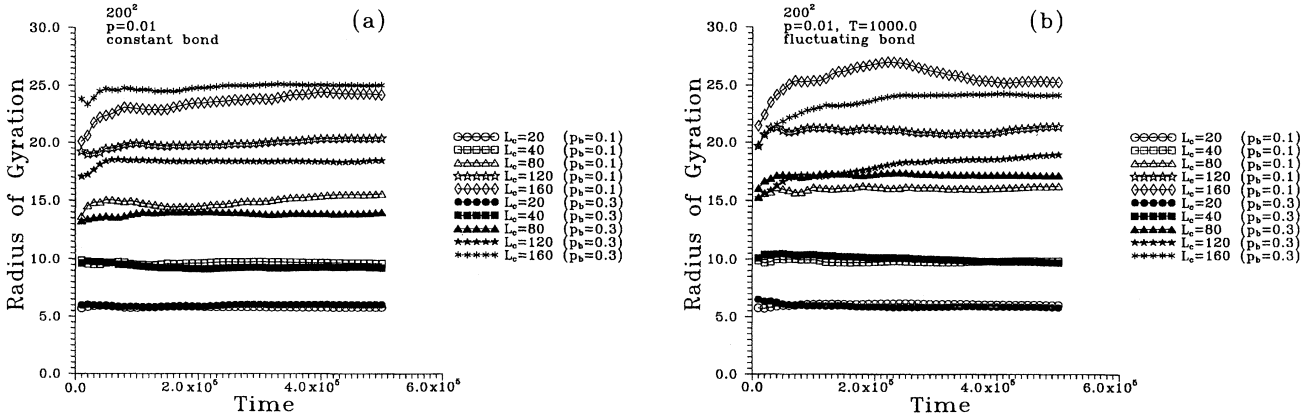

FIG. 15. Radius of gyration vs time of (a) constant bond chains and (b) fluctuating bond chains at $T=1000.0$, for chain lengths $L_c=20-160$ and barrier concentrations $p_b=0.1$ and 0.3. The lattice size was 200×200 with 30 independent samples.

any case, when the radius of gyration of the chains becomes comparable to the size of the pore in which it is placed, then the size of the chain conforms to the size of the pore, which is consistent with the general notion.

A similar effect of reduction in the radius of gyration for the long chains at higher barrier concentrations (low porosity) is also observed for the fluctuating bonds. However, the rate of decay of the radius of gyration with the chain length does not seem to be as abrupt as for the chains with the constant bonds. Thus, as long as the radius of gyration of the chain is smaller than the size of the host pores, the radius of gyration is not affected by the barriers; the probability of such an occurrence is high at low barrier concentration and for relatively short chains. At the high barrier concentration, on the other hand, the size of the chain seems to reduce in order to conform to the pore.

VI. SUMMARY AND CONCLUSION

We have presented a computer simulation study of the conformational and transport properties of polymer chains in a porous medium. We consider discrete lattices in two and three dimensions. The chains are modeled by constrained SAW. The initialization of the random sequential generation of chains is followed by the porous matrix, which is generated by distributing the impenetrable quenched barriers. We

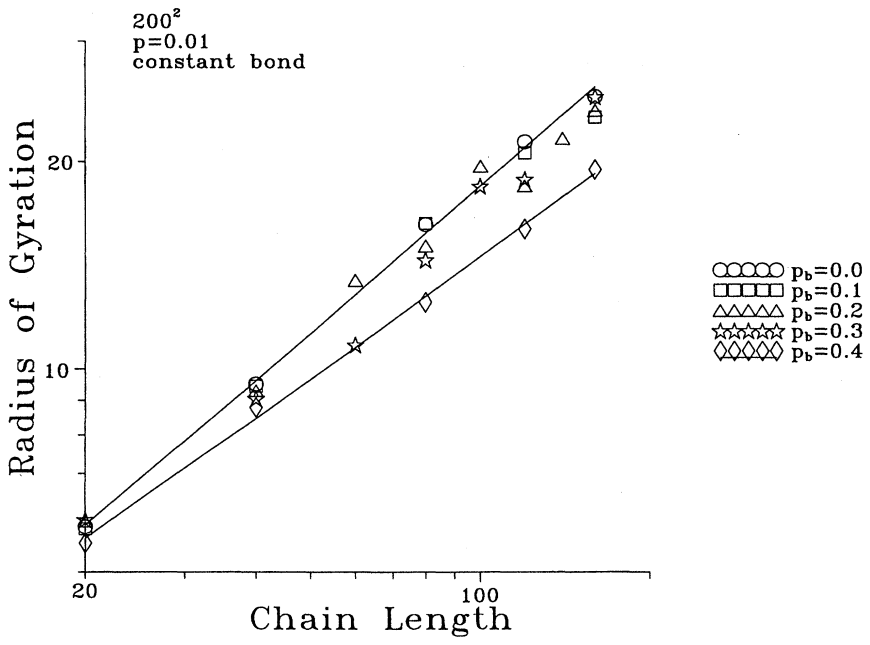

FIG. 16. Log-log plot of radius of gyration vs chain length of constant bond chains, at barrier concentrations $p_b=0.0-0.4$. Same statistics as in Fig. 15. The least square fit lines show the extreme values of exponent γ.

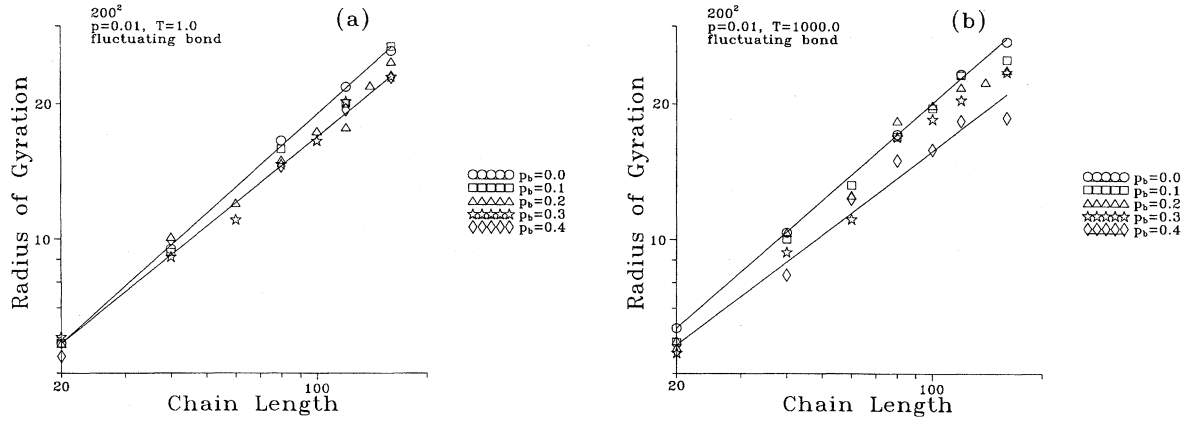

FIG. 17. Log-log plot of radius of gyration vs chain length of fluctuating bond chains at (a) $T=1.0$ and (b) $T=1000.0$ and barrier concentrations $p_b=0.0-0.4$. Same statistics as in Fig. 15. The least square fit lines show the extreme values of exponent γ.

consider two types of links between the consecutive nodes of the chains: (i) constant bond and (ii) flexible (fluctuating) bond. We have analyzed in detail the variation of the rms displacement of the chains with time, keeping track of the contributions due to reptation and kink-jump motion separately. The radius of gyration is also studied as the chains evolve through their conformational and translational relaxations. Effects of porosity or the concentration of barriers on these properties are explored and several unusual behaviors are observed.

In addition to normal global transport of chains, we observe unusual nondiffusive transport phenomena such as subdiffusive power-law dependence of the rms displacement ($R_{\rm rms}$) of the chain with time (t), i.e., $R_{\rm rms}=At^k$ at low porosity ($p_s=1-p_b$). In two dimensions, we find that the power-law exponent k is nonuniversal as it depends on the barrier concentration (p_b) and the chain length (L_c) with the magnitude of $k\simeq 0.0-0.5$. The vanishing magnitude of the exponent k at low porosity [below the percolation threshold (p_{sc}), $p_s<p_{sc}$] is not unexpected. However, low values of $k<0.5$ at high barrier concentrations or low porosities with the long ("infinite") connected pore are signatures of anomalouslike subdiffusive transport behavior. This power-law behavior is different from the well-known anomalous diffusion behavior of a stochastic motion of a particle in a percolating system in the sense that it depends on the chain length. The exponent k is found to be smaller for chains with higher lengths. Thus, our data seem to suggest a range of values for the exponent k. The chains with flexible bonds exhibit better relaxation with the value of k slightly higher than that for the chains with constant bonds at low porosities. The subdiffusion constant A shows a nonuniversal power-law dependence on the chain length, $A\sim L_c^{-\alpha}$ with $\alpha\simeq 0.28-1.85$ for chains with constant bonds, and $0.33-1.27$ for chains with flexible bonds. A similar but less pronounced effect of impurity barriers is also observed in three dimensions.

It is worth pointing out that in order to verify the crossover from Rouse to reptation dynamics, one usually looks at the dependence of the diffusion constant (D) on the chain length, $D\sim L_c^{-2}$. In our simulations, we do not consider short time dynamics since the motion of the end nodes dominates over the internal kink-jump; therefore, our result is valid for

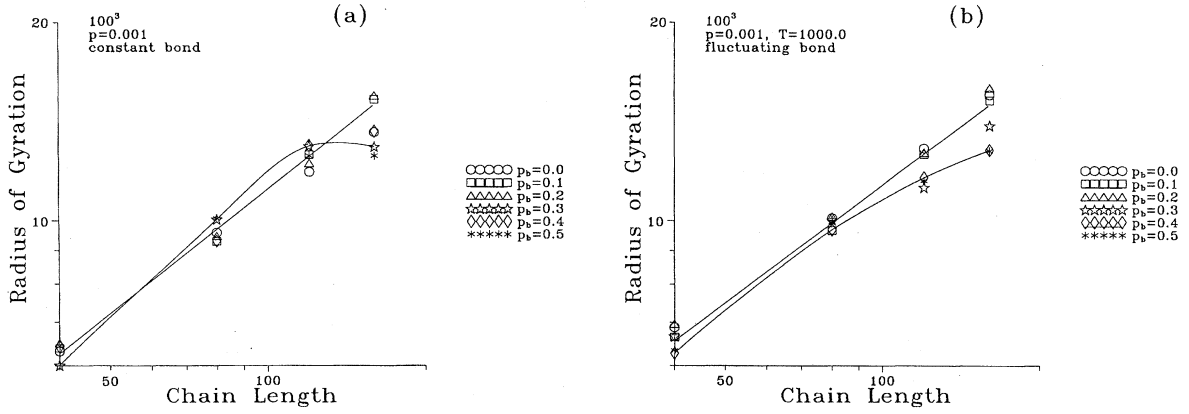

FIG. 18. Log-log plot of radius of gyration vs chain length of (a) constant bond chains and (b) fluctuating bond chains at $T=1000.0$, and barrier concentrations $p_b=0.0-0.5$. The lattice size was $100\times 100\times 100$ with 10 independent samples.

time regimes longer than reptation. In such long time regimes, we observe subdiffusive behavior which is nonuniversal as pointed out above.

The power-law variation of the radius of gyration of the chains with the contour length (mass) is affected by the barrier concentration of the barriers; characteristics of the crossover from a SAW to collapse conformations (in three dimensions) are reported along with the possibility of an anomalous conformation (in two dimensions) as a function of barrier concentration.

ACKNOWLEDGMENTS

This work was supported by a NSF-EPSCoR grant. Part of this work was prepared while R.B.P. was visiting Cologne University and the National University of Singapore. We acknowledge the generous support for computer time on the CRAY YMP at the Mississippi Center of Supercomputing Research and CRAY T3D at the Pittsburgh Supercomputing Center. We thank A. Baumgärtner and Rob Lescanec for useful discussion.

[1] P. J. Flory, *Principles of Polymer Chemistry* (Cornell University Press, Ithaca, 1953).
[2] J. D. Ferry, *Viscoelatic Properties of Polymers* (Wiley, New York, 1980).
[3] P. G. de Gennes, *Scaling Concepts in Polymer Physics* (Cornell University Press, Ithaca, 1979).
[4] M. Doi and S. F. Edwards, *The Theory of Polymer Dynamics* (Clarendon Press, Oxford, 1986).
[5] R. B. Pandey, J. Phys. A **19**, L53 (1986).
[6] T. P. Lodge, N. A. Rotstein, and S. Prager, Adv. Chem. Phys. **79**, 1 (1990).
[7] J. P. Skolnick and A. Kolinski, Adv. Chem. Phys. **78**, 223 (1990).
[8] A. Baumgartner, in *Application of Monte Carlo Simulation in Statistical Physics*, edited by K. Binder (Springer-Verlag, Berlin, 1986).
[9] J. M. Deutsch, Phys. Rev. Lett. **54**, 56 (1985).
[10] J. Noolandi *et al.*, Phys. Rev. Lett. **58**, 2428 (1987).
[11] G. S. Grest and K. Kremer, Phys. Rev. A **33**, 3628 (1986).
[12] K. Kremer, G. S. Grest, and I. Carmesin, Phys. Rev. Lett. **61**, 566 (1988).
[13] K. Kremer and G. S. Grest, J. Chem. Phys. **92**, 5057 (1990).
[14] K. Binder, in *Computational Modeling of Polymers*, edited by J. Bicerano (Marcel Dekker, New York, 1992), p. 221.
[15] K. Binder, in *Monte Carlo and Molecular Dynamics Simulations in Polymer Science*, edited by K. Binder (Oxford University Press, Clarendon, 1995).
[16] R. B. Pandey, Physica A **187**, 77 (1992).
[17] J. Becklehimer and R. B. Pandey, Phys. Rev. E **51**, 3341 (1995).
[18] M. Sahimi, Rev. Mod. Phys. **65**, 1393 (1993).
[19] D. Stauffer and A. Aharony, *Introduction to Percolation Theory* (Taylor and Francis, London, 1994).
[20] M. Sahimi, *Applications of Percolation Theory* (Taylor and Francis, London, 1994).
[21] R. B. Pandey and D. Stauffer, Phys. Rev. Lett. **52**, 527 (1983).
[22] S. Havlin and D. Ben-Avraham, Adv. Phys. **36**, 697 (1987).
[23] K. W. Kehr and K. Binder, in *Application of Monte Carlo Simulation in Statistical Physics*, edited by K. Binder (Springer-Verlag, Berlin, 1986).
[24] H. E. Stanley, I. Majid, A. Margolina, and A. Bunde, Phys. Rev. Lett. **53**, 1706 (1984).
[25] S. Alexander and R. Orbach, J. Phys. Lett. (Paris) **43**, L625 (1982).
[26] Y. Gefen and A. Aharony, Phys. Rev. Lett. **50**, 77 (1983).
[27] M. Wolfgardt, J. Baschnagel, and K. Binder, J. Phys. (Paris) **5**, 1035 (1995).
[28] M. Muthukumar, J. Chem. Phys. **90**, 4594 (1989).
[29] A. Baumgartner and M. Muthukumar, J. Chem. Phys. **87**, 3082 (1987).
[30] A. Baumgartner, Europhys. Lett. **4**, 1221 (1987).
[31] M. Muthukumar and A. Baumgartner, Macromolecules **22**, 1937 (1989).
[32] M. Muthukumar and A. Baumgartner, Macromolecules **22**, 1941 (1989).
[33] P. Haronska and T. A. Vilgis, J. Chem. Phys. **101**, 3104 (1994).
[34] F. Horkay, H. B. Stanley, E. Geissler, and S. M. King, Macromolecules **28**, 678 (1995).
[35] I. Carmesin and K. Kremer, Macromolecules **21**, 2819 (1988).
[36] E. S. Arvanitidou, D. Hoagland, and D. Smisek, Biopolymers **31**, 435 (1991).
[37] R. M. Briber, X. Liu, and B. J. Bauer, Science **268**, 395 (1995).
[38] D. A. Hoagland and E. S. Arvanitidou, Polymer Preprints **34**, 1059 (1993).
[39] G. M. Foo and R. B. Pandey, Phys. Rev. E **51**, 5738 (1995).
[40] A. R. Volkel and J. Noolandi, J. Chem. Phys. **102**, 5506 (1995).
[41] J. Baschnagel and K. Binder, Physica A **204**, 47 (1994).
[42] R. Lambourne, *Paint and Surface Coatings* (Ellis Horwood, Chichester, 1987).
[43] J. Becklehimer and R. B. Pandey, J. Stat. Phys **75**, 765 (1994).
[44] H. Nakanishi and J. Moon, Physica A **191**, 309 (1992).